Continuous-time quantum walks on one-dimensional regular networks

Xin-Ping Xu*
Institute of Particle Physics, HuaZhong Normal University, Wuhan 430079, China
Institute of High Energy Physics, Chinese Academy of Science, Beijing 100049, China
(Received 22 November 2007; revised manuscript received 24 March 2008; published 19 June 2008)

In this paper, we consider continuous-time quantum walks (CTQWs) on a one-dimensional ring lattice of N nodes in which every node is connected to its $2m$ nearest neighbors (m on either side). In the framework of the Bloch function ansatz, we calculate the space-time transition probabilities between two nodes of the lattice. We find that the transport of CTQWs between two different nodes is faster than that of the classical continuous-time random walks (CTRWs). The transport speed, which is defined by the ratio of the shortest path length and propagating time, increases with the connectivity parameter m for both CTQWs and CTRWs. For fixed parameter m, the transport of CTRWs gets slower with the increase of the shortest distance while the transport (speed) of CTQWs turns out to be a constant value. In the long-time limit, depending on the network size N and connectivity parameter m, the limiting probability distributions of CTQWs show various patterns. When the network size N is an even number, the probability of being at the original node differs from that of being at the opposite node, which also depends on the precise value of parameter m.

DOI: 10.1103/PhysRevE.77.061127 PACS number(s): 05.60.Gg, 03.67.−a, 05.40.−a, 05.60.Cd

I. INTRODUCTION

Quantum walks have important applications in various fields of solid-state physics, polymer chemistry, biology, astronomy, mathematics, and computer science [1–6]. A quantum random walk (QRW) is a natural extension to the quantum world of the ubiquitous classical random walk. It was first introduced in [7] and extensively investigated recently in connection with possible applications to quantum algorithms [8]. The behavior of quantum walks differs from that of classical random walks in several striking ways, due to the fact that quantum walks exhibit interference patterns whereas the classical random walks do not. For instance, the mixing times, hitting times, and exit probabilities of quantum walks can differ significantly from those of analogously defined random walks [9–11]. In recent years, two types of quantum walks exist in the literature: discrete-time quantum coined walks and continuous-time quantum walks [12,13]. Although both types of quantum walks have efficient quantum algorithms with respect to their classical counterparts, quantum walks show some advantages in dealing with decoherence processes compared to the discrete-time quantum algorithms, which are very sensitive to environmental quantum noise [14].

Here, we focus on continuous-time quantum walks (CTQWs). Most previous studies consider CTQWs on simple structures, such as the line [15,16], cycle [17,18], hypercube [19], Cayley tree [20], dendrimer [21], and other regular networks with simple topology. Although CTQWs have received much attention and there has been some work about CTQWs on general graphs, many questions about CTQWs appear to be quite difficult to answer at the present time. For simple structures these quantum walks are analytically solvable and directly related to well-known problems in solid state physics. Recently, Mülken *et al.* have studied the space-time structures of CTQWs on one- and two-dimensional lattices with periodic boundary conditions [22,23]. The topology of the lattices they considered is oversimplified, i.e., each node is only connected to its two nearest neighbors. For regular graphs with symmetrical structure, the dynamics of the quantum transport is determined by the topology of the network. To this end, it is natural to consider quantum transport on general lattices with more connectivity.

In this paper, we study CTQWs on a one-dimensional ring lattice of N nodes in which every node is connected to its $2m$ nearest neighbors (m on either side). This generalized regular network has broad applications in various coupled dynamical systems, including biological oscillators [24], Josephson junction arrays [25], neural networks [26], synchronization [27], small-world networks [28], and many other self-organizing systems. We analyze quantum walks on such general networks with periodic boundary conditions using the Bloch function approach [29], which is commonly used in solid-state physics. We derive analytical expressions for the transition probabilities between two nodes of the networks, and compare them with the results of continuous-time random walks (CTRWs).

The paper is structured as follows: In Sec. II we review the properties of CTQWs presented in Ref. [30] and give the exact solutions to the transition probabilities on the general ring network. Section III presents the time evolution of the probabilities. In Sec. IV, we consider the distributions of long-time limiting probabilities. Conclusions and discussions are given in the last part, Sec. V.

II. CONTINUOUS-TIME QUANTUM WALKS

Keeping in line with previous results on quantum walks, we study continuous-time quantum walk on networks and compare the results with the classical counterparts.

*xuxp@mail.ihep.ac.cn

A. Continuous-time quantum walks on general networks

We consider a walk on a general graph, which is a collection of connected nodes and simple links without weight and directions. The topology of such simple graphs can be described by the corresponding Laplace matrix A. The nondiagonal elements A_{ij} are equal to -1 if nodes i and j are connected and 0 otherwise. The diagonal elements A_{ii} equal the number of total links connected to node i, i.e., A_{ii} equals the degree of node i. Classically, the evolution of continuous-time random walk is governed by the master equation [3]

$$\frac{dp_{k,j}}{dt} = \sum_l T_{kl} p_{l,j}(t), \tag{1}$$

where $p_{k,j}(t)$ is the conditional probability to find the CTRW at time t at node k when starting at node j. The matrix T is the transfer matrix of the walk, and is related to the Laplace matrix by $T=-\gamma A$. Here, for the sake of simplicity, we assume the transmission rate γ for all connections to be equal. Then the solution of the above equation is

$$p_{k,j}(t) = \langle k|e^{tT}|j\rangle. \tag{2}$$

Quantum mechanically, the dynamical evolution equation of continuous-time quantum walks is obtained by replacing the Hamiltonian of the system by the classical transfer matrix, $H=-T$ [9,10]. The states $|j\rangle$ endowed with the nodes j of the network form a complete, orthonormalized basis set, which span the whole accessible Hilbert space, i.e., $\Sigma_k|k\rangle\langle k|=1$, $\langle k|j\rangle=\delta_{kj}$. The time evolution of state $|j\rangle$ is given by the Schrödinger equation (SE)

$$i\frac{d|j\rangle}{dt} = H|j\rangle, \tag{3}$$

where the mass $m\equiv 1$ and $\hbar\equiv 1$ is assumed in the above equation. Starting at time t_0 from the state $|j\rangle$, the evolution equation of the state $|j\rangle$ is $|j,t\rangle=U(t,t_0)|j\rangle$, where $U(t,t_0)=e^{-iH(t-t_0)}$ is the quantum mechanical time evolution operator. The transition amplitude $\alpha_{k,j}(t)$ from state $|j\rangle$ at time 0 to state $|k\rangle$ at time t is

$$\alpha_{k,j}(t) = \langle k|e^{-itH}|j\rangle. \tag{4}$$

Combining Eq. (3), we have

$$i\frac{d\alpha_{k,j}}{dt} = \sum_l H_{kl}\alpha_{l,j}(t). \tag{5}$$

We note the different normalization for CTRWs and CTQWs. For CTRWs, $\Sigma_k p_{k,j}=1$ and quantum mechanically $\Sigma_k|\alpha_{k,j}|^2=1$ holds.

To get the exact solution of Eqs. (1) and (5), all the eigenvalues and eigenvectors of the transfer operator and Hamiltonian are required. We use E_n to represent the nth eigenvalue of A and denote the orthonormalized eigenstate of Hamiltonian by $|q_n\rangle$, such that $\Sigma_n|q_n\rangle\langle q_n|=1$. The classical transition probability between two nodes is given by

$$p_{k,j}(t) = \sum_n e^{-\gamma t E_n}\langle k|q_n\rangle\langle q_n|j\rangle, \tag{6}$$

and the quantum mechanical transition probability between k and j is

$$\pi_{k,j}(t) = |\alpha_{k,j}(t)|^2 = \sum_{n,l} e^{-i\gamma t(E_n-E_l)}\langle k|q_n\rangle\langle q_n|j\rangle\langle j|q_l\rangle\langle q_l|k\rangle. \tag{7}$$

For finite networks, $\pi_{k,j}(t)$ do not decay ad infinitum but at some time fluctuate about a constant value. This value is determined by the long-time average of $\pi_{k,j}(t)$

$$\begin{aligned}\chi_{k,j} &= \lim_{T\to\infty}\frac{1}{T}\int_0^T \pi_{k,j}(t)dt \\ &= \sum_{n,l}\langle k|q_n\rangle\langle q_n|j\rangle\langle j|q_l\rangle\langle q_l|k\rangle \lim_{T\to\infty}\frac{1}{T}\int_0^T e^{-i\gamma t(E_n-E_l)}dt \\ &= \sum_{n,l}\delta_{E_n,E_l}\langle k|q_n\rangle\langle q_n|j\rangle\langle j|q_l\rangle\langle q_l|k\rangle.\end{aligned} \tag{8}$$

B. Continuous-time quantum walks on a one-dimensional ring lattice and Bloch ansatz solutions

In the subsequent calculation, we restrict our attention to CTQWs on general one-dimensional (1D) ring lattices with periodic boundary conditions. The network is organized in a very regular manner, i.e., each node of the lattice is connected to its $2m$ nearest neighbors (m on either side); thus the Laplace matrix A takes the form

$$A_{ij} = \begin{cases} 2m & \text{if } i=j, \\ -1 & \text{if } i=j\pm z,\ z\in[1,m], \\ 0 & \text{otherwise.}\end{cases} \tag{9}$$

The Hamiltonian of the system is given by $H=\gamma A$. For simplicity of analytical treatment, we set $\gamma=1$ in further calculations. The Hamiltonian acting on the state $|j\rangle$ can be written as

$$H|j\rangle = (2m+1)|j\rangle - \sum_{z=-m}^{m}|j+z\rangle, \quad z\in \text{integers}. \tag{10}$$

The above equation is the discrete version of the Hamiltonian for a free particle moving on the lattice. Using the Bloch function approach [29] for the periodic system in solid-state physics, the time-independent SE reads

$$H|\psi_n\rangle = E_n|\psi_n\rangle. \tag{11}$$

The Bloch states $|\psi_n\rangle$ can be expanded as a linear combination of the states $|j\rangle$ localized at node j,

$$|\psi_n\rangle = \frac{1}{\sqrt{N}}\sum_{j=1}^{N} e^{-i\theta_n j}|j\rangle. \tag{12}$$

Substituting Eqs. (10) and (12) into Eq. (11), we obtain the eigenvalues (or energy) of the system,

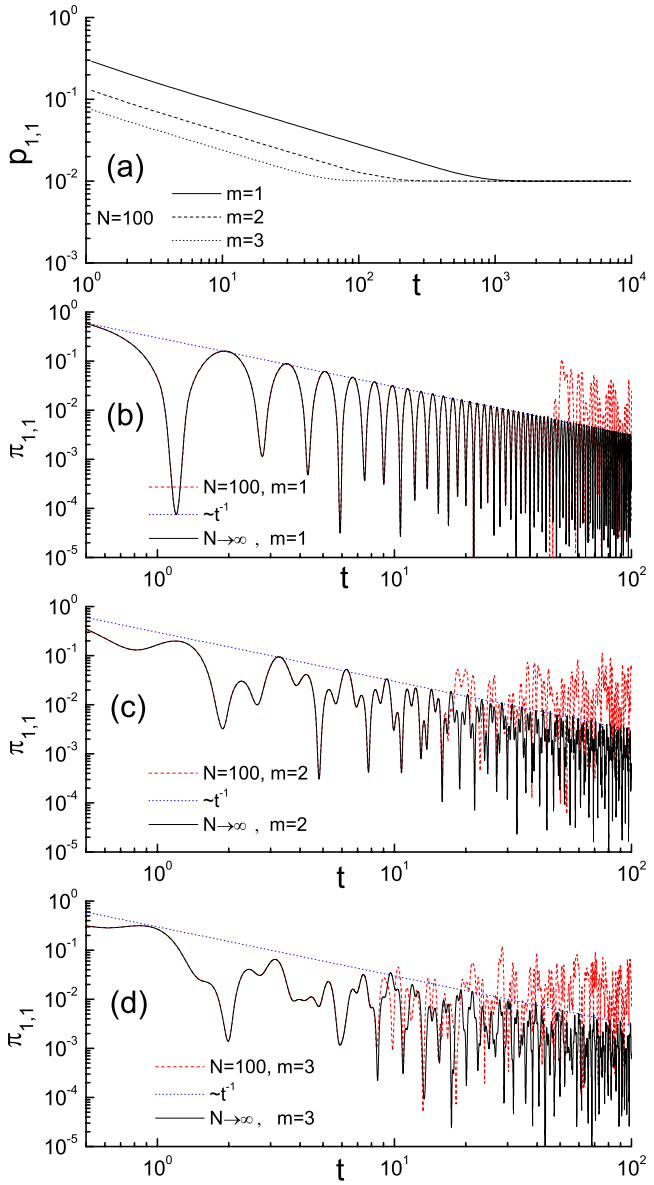

FIG. 1. (Color online) Evolution of the probability of being at the initial node 1. (a) Classical return probability $p_{1,1}$ on networks of $N=100$ with different values of m. $p_{1,1}$ approaches the equipartitioned probability $1/N$ quickly on networks with high connectivity. (b)–(d) show the evolution of quantum mechanical return probabilities $\pi_{1,1}$ with $m=1$–3, respectively. The dashed curves are results on a network of size $N=100$ according to Eq. (20); the solid curves are the corresponding results on infinite networks according to Eq. (17). The dashed lines show the scaling behavior $\pi_{1,1} \sim t^{-1}$.

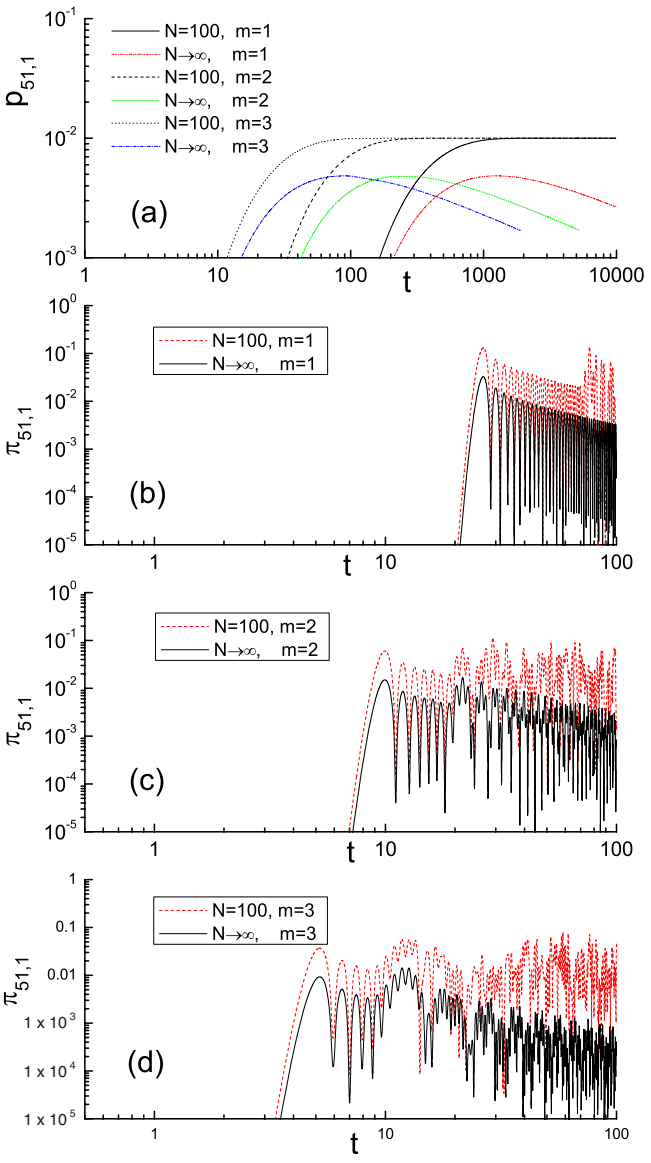

FIG. 2. (Color online) Evolution of the probability of finding the walker at the opposite node 51 when the initial node is 1. (a) Classical transition probability $p_{51,1}$ for infinite networks and finite network of $N=100$ with different parameters m. We can see that the probability on an infinite network with large connectivity reaches its maximum more quickly than that on an infinite network with small connectivity. (b)–(d) are the quantum mechanical transition probabilities $\pi_{51,1}$ for $m=1$–3. The solid curves are the results on infinite networks; the dashed curves are the results on finite networks of $N=100$.

$$E_n = 2m - 2\sum_{j=1}^{m} \cos(j\theta_n). \tag{13}$$

The periodic boundary condition for the network requires that the projection of the Bloch states $|N+1\rangle$ equals that on the state $|1\rangle$; thus $\theta_n = 2n\pi/N$ with n integer and $n \in [0, N)$. Replacing $|q_n\rangle$ by the Bloch states $|\psi_n\rangle$ in Eqs. (6) and (7), we can get the classical and quantum transition probabilities

$$p_{k,j}(t) = \frac{1}{N}\sum_n e^{-tE_n} e^{-i(k-j)2n\pi/N}, \tag{14}$$

$$\pi_{k,j}(t) = |\alpha_{k,j}(t)|^2 = \frac{1}{N^2}\sum\nolimits_{n,l} e^{-it(E_n - E_l)} e^{-i(k-j)(n-l)2\pi/N}. \tag{15}$$

For infinite networks, i.e., $N \to \infty$, Eqs. (14) and (15) translate to

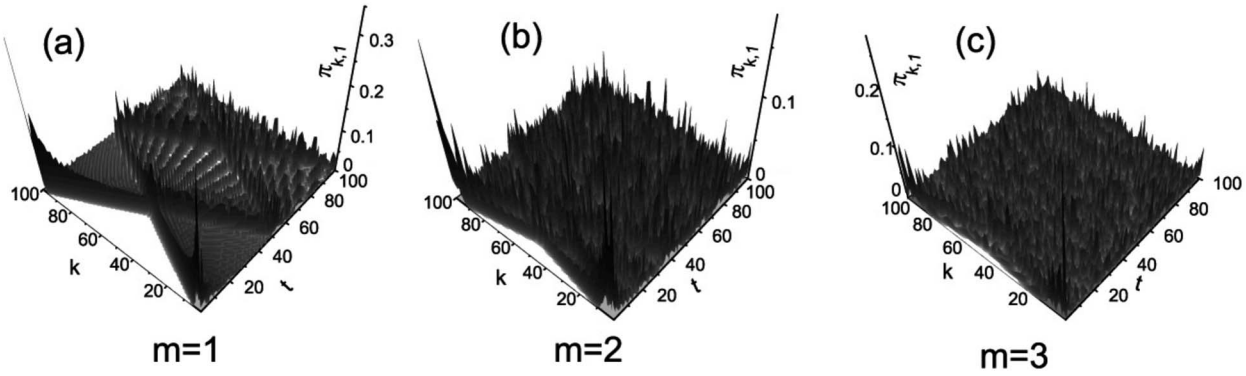

FIG. 3. Development of transition probabilities $\pi_{k,1}(t)$ for CTQWs on a network of $N=100$ with parameter $m=1$ (a), 2 (b), and 3 (c). The initial exciton starts at node 1.

$$\lim_{N\to\infty} p_{k,j}(t) = \frac{e^{-2mt}}{2\pi}\int_{-\pi}^{\pi} e^{-i\theta(k-j)}\exp\left(2t\sum_{j=1}^{m}\cos j\theta\right)d\theta, \tag{16}$$

$$\lim_{N\to\infty} \pi_{k,j}(t) = \left|\frac{1}{2\pi}\int_{-\pi}^{\pi} e^{-i\theta(k-j)}\exp\left(2it\sum_{j=1}^{m}\cos j\theta\right)d\theta\right|^2. \tag{17}$$

In particular, when $m=1$, the network corresponds to a cycle graph where each node has exactly two nearest neighbors. The limiting transition probabilities can be rewritten as $\lim_{N\to\infty} p_{k,j}(t)=e^{-2t}J_{k-j}(2t)$ and $\lim_{N\to\infty} \pi_{k,j}(t)=[J_{k-j}(2t)]^2$, where $J_n(x)$ is the Bessel function of the first kind [31]. This is consistent with the result in Ref. [23]. The difference between finite and infinite networks is that for infinite networks the interference of quantum transport is weak compared to that in finite networks. For larger values of m, the above analytical expression cannot be further simplified. We can calculate the transition probabilities directly using integration for infinite networks. We will show that there is some difference of the transition probabilities between finite and infinite networks at long time scales.

Finally, the long-time-averaged probability between two nodes yields

$$\chi_{k,j} = \frac{1}{N^2}\sum_{n,l}\delta_{E_n,E_l}e^{-i(k-j)(n-l)2\pi/N}. \tag{18}$$

Interestingly, the long-time-averaged probability is related to the spectrum of the network. This is in contrast to the classical transport, where there is a uniform probability $(1/N)$ to find the walker at every node. The time-limiting probabilities depend on the degeneracies of the eigenvalues, which result in odd, unexpected patterns of the limiting probability distributions.

III. TIME EVOLUTION OF THE PROBABILITIES

In this section, we analyze the time-dependent probabilities of the theoretical calculations. The numerical determination of the eigenvalues, eigenvectors and integration is done using the software MATHEMATICA. Specifically, we perform our calculations on infinite and finite ($N=100$) networks with different connectivities m.

A. Return probabilities

The probability to be still or again at the initial node is a good measure to quantify the efficiency of the transport [32]. Classically, according to Eq. (14), the probability of being at the original node j is

$$p_{j,j}(t) = \frac{1}{N}\sum_{n} e^{-tE_n}, \tag{19}$$

which depends only on the eigenvalues. The quantum mechanical probability of finding the walker at the initial node is given by Eq. (15),

$$\pi_{j,j}(t) = \frac{1}{N^2}\sum_{n,l} e^{-it(E_n-E_l)}, \tag{20}$$

which also depends on the eigenvalues of the system. The return probability is independent of the position of the initial excitation nodes because of the symmetry of the network topology. Analogously, employing the relation $k=j$, we can calculate the return probabilities on infinite networks according to Eqs. (16) and (17).

Figure 1 shows the return probabilities for CTRWs and CTQWs. Consider a CTRW on a network of size $N=100$ and assume that the initial excitation starts at node 1. Figure 1(a) depicts the temporal behavior of the return probability with different values of m. There is a power-law decay ($p \sim t^{-0.5}$) at the beginning of the transport, but after some time p reaches a constant value. This time is determined by the time when $p_{1,1}$ reaches the equipartitioned probability $1/N$. The time becomes smaller when the parameter m increases; this indicates that it takes less time for the return probability to reach the equipartitioned probability on networks with high connectivity. Figures 1(b)–1(d) show the quantum mechanical return probabilities for $m=1$, 2, and 3, respectively. The dashed curves show the results on network of $N=100$ and the black solid curves show the results on infinite networks according to Eq. (17). The dashed lines indicate the

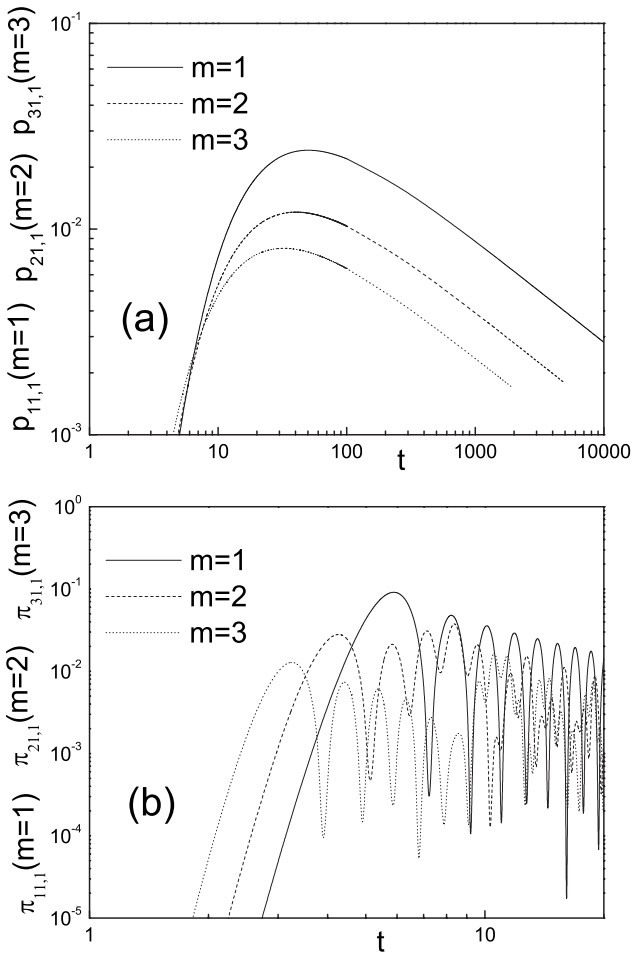

FIG. 4. Time evolution of transition probabilities on infinite networks for CTRWs (a) and CTQWs (b). The initial excitation is located at node 1. The solid curves show the probabilities of being at node 11 for $m=1$ [$p_{11,1}$ in (a) and $\pi_{11,1}$ in (b)]. Dashed curves show the probabilities of being at node 21 for $m=2$ [$p_{21,1}$ in (a) and $\pi_{21,1}$ in (b)]. Dotted curves show the probability of being at node 31 for $m=3$ [$p_{31,1}$ in (a) and $\pi_{31,1}$ in (b)]. The shortest path lengths between the two nodes are equal, but the time when the first maximal value appears are different.

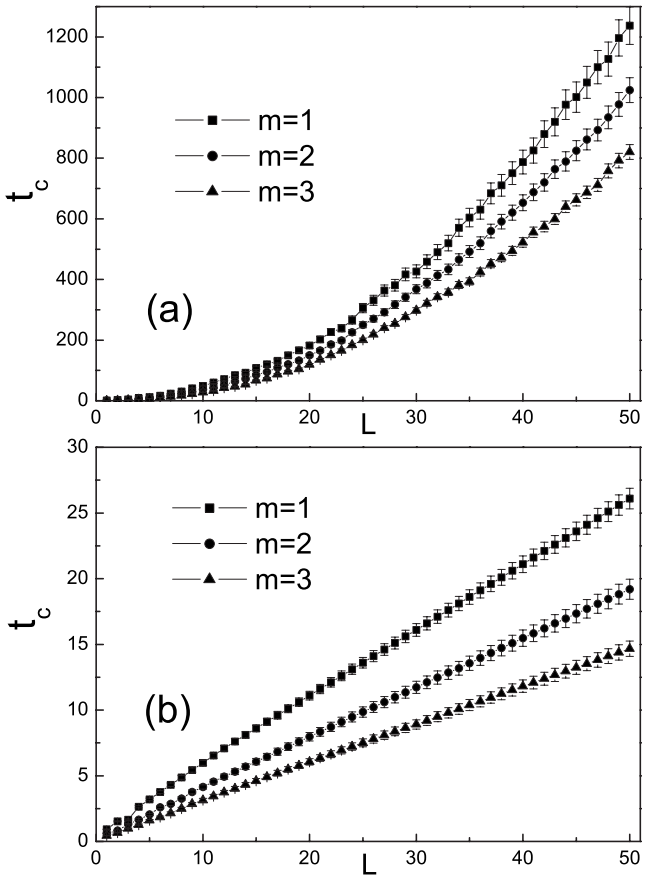

FIG. 5. Characteristic time t_c as a function of the shortest path length L with different values of m for CTRWs (a) and CTQWs (b). From the figure, we can see that the classical transport gets slower while the quantum transport velocity turns out to be invariable for a certain value of m.

scaling behavior $\pi_{1,1} \sim t^{-1}$. We note that the return probabilities of finite and infinite networks agree with each other on small time scales. At later times waves propagating on finite networks start to interfere; this leads to different probabilities and the deviation happens at earlier times on highly connected networks (with larger values of m). Furthermore, the return probabilities oscillate frequently on highly connected networks and there are more peaks compared to networks with small values of m. Such behavior may be attributed to the fact that the interferences on networks with high connectivity are stronger than on those with small connectivity.

B. Transition probabilities and transport velocity

The transition probabilities between two different nodes provide us more information about the transport process over the whole network. For a finite network of $N=100$, we consider the probability of finding the walker at the opposite node. Figure 2 shows the transition probabilities for CTRWs and CTQWs. Figure 2(a) shows the classical transition probabilities $p_{51,1}$ on infinite and finite networks of size $N=100$ with different values of m. As we can see, the transition probabilities on finite networks with more connectivity approach the equipartitioned probability $1/N$ more quickly than those on networks with less connectivity. For infinite networks, the transition probabilities increase with time in the first period, and then reach a maximum and decrease on the large time scale. Quantum mechanically, the transition probabilities for $m=1$–3 are shown in Figs. 2(b)–2(d). The dashed curves are the results for networks of $N=100$; the solid curves are the corresponding results for infinite networks. The transition probabilities on infinite networks are smaller than those on finite networks at the same time. Interestingly, for the same connectivity parameter m, the characteristic time t_c when the first maximum of the probabilities occurs on finite networks equals that on infinite networks, i.e., the characteristic time t_c is independent of the size of the network.

The probabilities to go from a starting node to all other nodes at time t on a network of size $N=100$ with different values of m are plotted in Fig. 3. The starting excitation is located at node 1, and we can see that the time taken to propagate to the opposite node 51 becomes small on net-

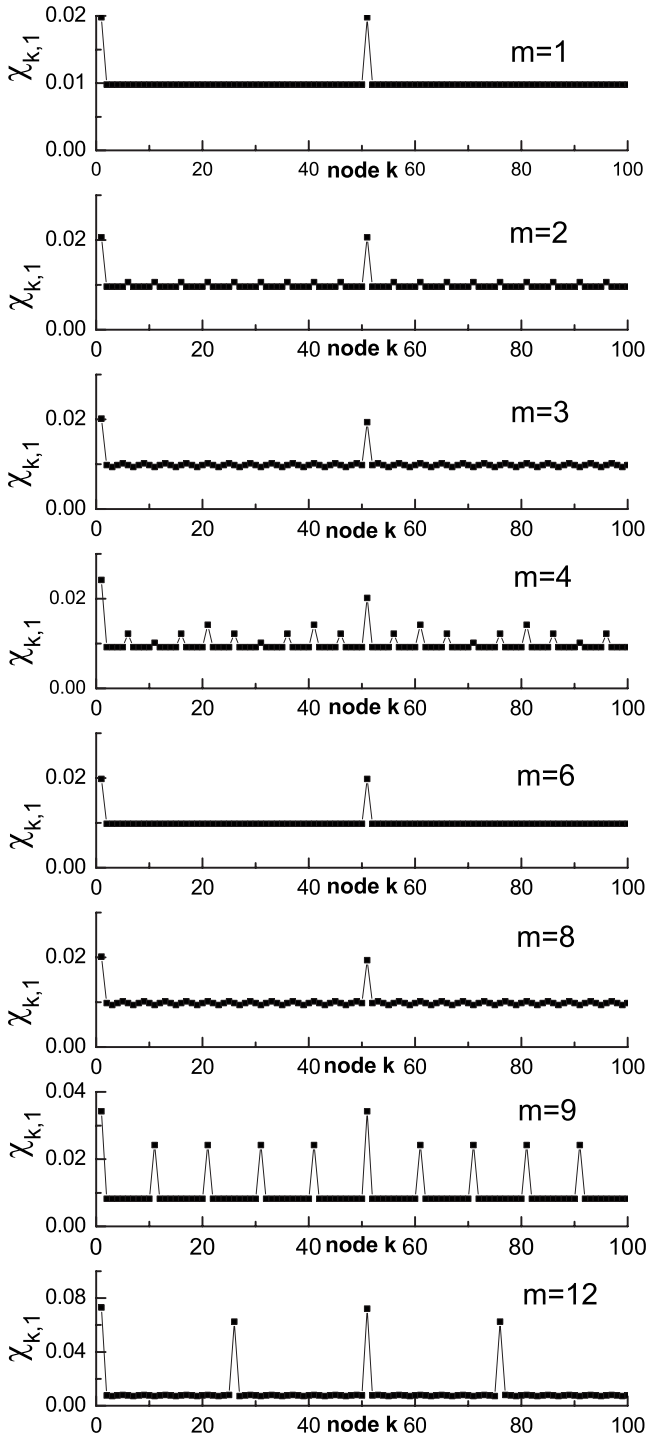

FIG. 6. Long-time-averaged probability distribution $\chi_{k,1}$ for CTQWs on networks of size $N=100$ with different values of m.

works with large values of m. In addition, the structure is quite regular when $m=1$. As m increases, the pattern becomes irregular.

In order to compare the transport speed on different networks, we define the characteristic time t_c as the time when the first maximum of the probabilities occurs on infinite networks. This definition holds for both classical and quantum transport. For classical transport, there is only one maximal value and the characteristic time corresponds to the time when the equipartitioned probability $1/N$ is reached on finite networks. Now it is natural to ask the question: Does the transport take equal time between two nodes of the same shortest path length? To address this question, we calculate the transition probabilities between two nodes having the same value of the shortest path length on infinite networks. Figure 4(a) shows the classical transition probabilities $p_{11,1}$, $p_{21,1}$, and $p_{31,1}$ for $m=1$, $m=2$, and $m=3$. The shortest path lengths of the two nodes for the three infinite networks equal to 10, but the characteristic time t_c is small for highly connected networks. This indicates that the transport is quick on networks with high connectivity for CTRWs. For CTQWs, the same conclusion is also true, as confirmed by the corresponding plot in Fig. 4(b). The characteristic time t_c for the quantum transport is much smaller than that of the classical one; this supports the fact that the quantum walks have efficient quantum algorithms with respect to their classical counterparts [33].

Figure 5 shows the characteristic time t_c versus the shortest path length on networks with different values of m. For classical transport [Fig. 5(a)], t_c grows faster than the shortest path length L. It is found that the relationship between the characteristic time t_c and the shortest path length L can be well described by the quadratic equation $t_c=\beta L^2$, where the parameter β can be obtained by fitting the data. Defining the transport speed v as the ratio of L and t_c, we find that the classical transport speed becomes slow for large L, while the quantum transport speed turns out to be a constant value. We note that the transport speed v is large on highly connected networks even when the two nodes are located at the same distance $L_{i,j}$. By fitting the relation between t_c and L, we can estimate the quantum transport velocities for $m=1$, 2, and 3, respectively. The different behavior of the transport velocities between CTRQs and CTQWs is a striking characteristic that distinguishes the classical and quantum transport processes.

IV. LONG-TIME LIMITING PROBABILITIES

Now we consider the long-time-averaged probabilities. Classically, the long-time probabilities equal the equipartitioned probability $1/N$ [23]. Quantum mechanically, the limiting probabilities are determined by Eq. (18) but the situation is more complex for different network parameters. For $m=1$, the spectrum (or energy) of the system is $E_n=2-2\cos(\theta_n)$, where $\theta_n=2n\pi/N$, $n\in[0,N)$. If the network size N is an even number, there are two nondegenerate eigenvalues $E_{N/2}=4$ and $E_0=0$, and the other eigenvalues have degeneracy 2. The limiting probabilities can be written as

$$\chi_{ij}=\begin{cases}2(N-1)/N^2 & \text{if } i=j,\ i=j\pm N/2,\\ (N-2)/N^2 & \text{otherwise.}\end{cases} \tag{21}$$

If the network size N is an odd number, there is one nondegenerate eigenvalue $E_N=0$, and the other eigenvalues have degeneracy 2. The limiting probabilities can be summarized as

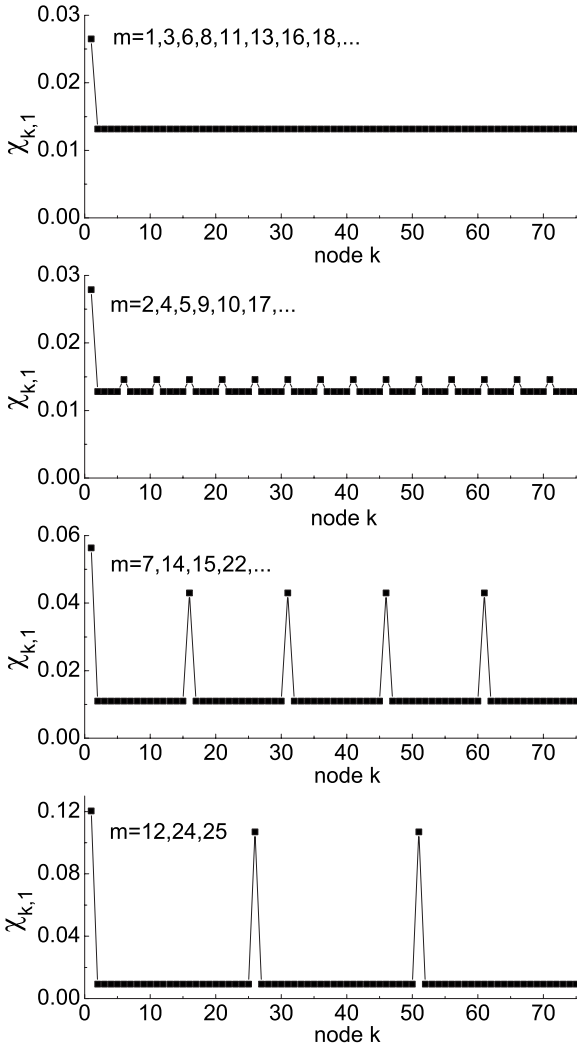

FIG. 7. Quantum mechanical limiting probabilities $\chi_{k,1}$ on networks of size $N=75$ with different values of m.

$$\chi_{ij} = \begin{cases} (2N-1)/N^2 & \text{if } i=j, \\ (N-1)/N^2 & \text{otherwise,} \end{cases} \tag{22}$$

which confirms the results in Ref. [30].

For other values of m, the limiting probability distributions can also be determined according to the degeneracy distribution of the eigenvalues, but this process is complicated for large values of m. Here, we report the limiting probabilities numerically obtained using Eq. (18). In Fig. 6, we display the limiting probabilities on a network of size $N=100$ with the starting node 1. As we can see, the probabilities for $m=6$ and 8 are the same as for $m=1$ and 3. After a careful examination, we find that $m=8$ and 3 have the same degeneracy distribution of eigenvalues, and $m=6$ and 1 have the same degenerate eigenvalue distribution. In particular, for all the values of m, there is a large probability to be still or again at the initial node and at the opposite node $k=51$. For some values of m, the probabilities at the two positions are extremely high, for instance, when $m=12$, the return probabilities exceed 0.07. For an odd network size, there is a higher probability to find the walker at the initial node than

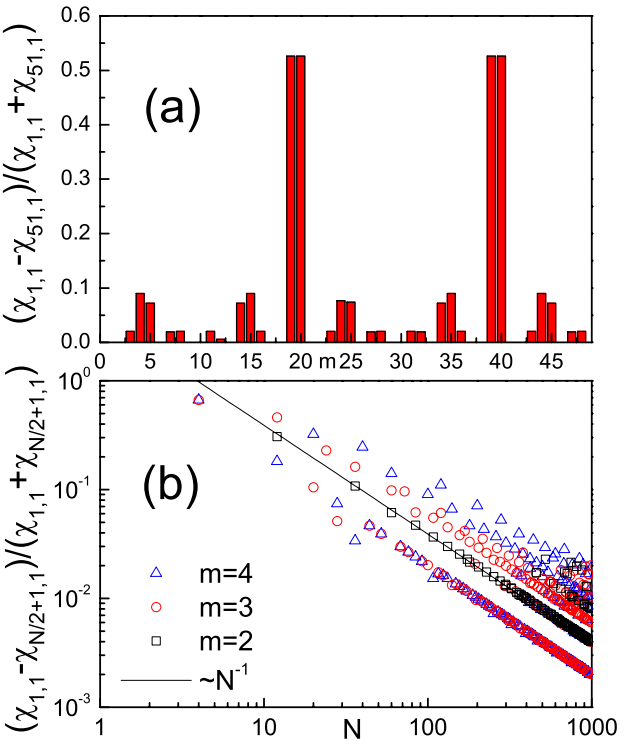

FIG. 8. (Color online) (a) Relationship between the quantity $\Delta(1,50) \equiv (\chi_{1,1}-\chi_{51,1})/(\chi_{1,1}+\chi_{51,1})$ and m on a network of size $N=100$. A nonzero value of $\Delta(1,50)$ represents asymmetry of probabilities $\pi_{1,1}$ and $\pi_{51,1}$. (b) $\Delta(1,N/2) \equiv (\chi_{1,1}-\chi_{N/2+1,1})/(\chi_{1,1}+\chi_{N/2+1,1})$ versus network size N for different values of m. The solid line indicates the power-law decay $\Delta(1,N/2) \sim N^{-1}$.

that at other nodes. For networks of size $N=101$ and $m<50$, the limiting probability distribution shows the same pattern described in Eq. (22). One may conjecture that the pattern of $\chi_{k,1}$ does not change when increasing the parameter m on odd-numbered networks, but this is not true for some values of network size N. For instance, on networks of size $N=75$ with some particular values of m, the limiting probability distribution differs from the pattern of Eq. (22) (see Fig. 7). It is interesting to note that the patterns of $\chi_{k,1}$ are the same for some values of m; this feature can be explained by the identical degeneracy distribution of the eigenvalues for different values of m.

As we have shown, if the network size N is an even number, there are high probabilities to find the walker at the initial node and the opposite node. For some values of m, we find that the probability of being at the initial node equals the probability of being at the opposite node. However, for some other values of m, this is not true. In Ref. [30], the authors find asymmetry of the probabilities for the starting node and its mirror node; their definition of the mirror node is based on the geometric symmetry of the network. In this paper, we define the mirror node i' of a given node i to be its opposite node, i.e., $i'=i+N/2$. We find asymmetry of the probabilities of being at the initial node and at the opposite node (mirror node) for some particular network parameters N and m. This asymmetry is small and not easily observed in Fig. 6. For a network of size $N=100$ and assuming the initial exciton starts at node 1, we find that asymmetries occur at m

$=3,4,5,7,8,11,12,14,15,16,19,20,\ldots$. The asymmetric limiting probabilities are particularly characterized by the difference between $\chi_{1,1}$ and $\chi_{51,1}$; thus we use the quantity $\Delta(1,50) \equiv (\chi_{1,1}-\chi_{51,1})/(\chi_{1,1}+\chi_{51,1})$ to detect the asymmetry of the probabilities. In Fig. 8(a), we present $\Delta(1,50)$ as a function of parameter m. There are 29 distinct values of m having asymmetric probabilities, which is indicated by the nonzero value of $\Delta(1,50)$.

To reveal the general dependence of the asymmetry on the network parameters, we plot the quantity $\Delta(1,N/2) \equiv (\chi_{1,1} - \chi_{N/2+1,1})/(\chi_{1,1}+\chi_{N/2+1,1})$ as a function of the network size N for different values of m, which are shown in Fig. 8(b). For $m=1$, the probabilities are symmetrical for all the network sizes N; thus we show only the asymmetry for $m=2$, 3, and 4. We find that the points break into several clusters, where some clusters $\Delta(1,N/2)$ decrease with increasing network size N as a power law: $\Delta(1,N/2) \sim N^{-1}$.

Except for the asymmetrical probabilities between the initial node and the opposite node (mirror node), we also find asymmetrical probabilities between other nodes and their mirror nodes. In our calculations, we find that such asymmetries can be different from the asymmetry of the probability of being at the initial node and being at its opposite node. For instance, considering a CTQW on a network of size $N=100$ and assuming that the initial excitation starts at node 1, there are asymmetries between $\chi_{1+n,1}$ and $\chi_{51+n,1}$ (n is an even number) for some values of m. The discrete values of m for different asymmetries can differ from each other, depending on the precise value of N and m. This situation is even more complex and requires further study.

V. CONCLUSIONS AND DISCUSSION

In summary, we have studied continuous-time quantum walks on a one-dimensional ring lattice of N nodes in which each node is connected to its $2m$ nearest neighbors (m on either side). Using the Bloch function approach, we calculate transition probabilities between two nodes of the lattice, and compare the results with those for the classical counterpart. It is found that the transport of a CTQW is faster than that of the classical continuous-time random walk. We define the transport velocity as the ratio of the shortest path length and spreading time between two nodes. For networks with a given parameter m, the transport of CTRWs gets slow with the increase of the shortest distance, while the transport of CTQWs spreads the network constantly. In the long-time limit, depending on the network parameters N and m, the limiting probability distributions of CTQWs show various patterns. When the network size N is an even number, the probability of being at the original node differs from that of being at the opposite node, which also depends on the precise value of the parameter m. Asymmetrical probabilities between other nodes and their mirror nodes also exist for some particular network parameters.

The asymmetry of the limiting probabilities of being at a node and being at its mirror node is an interesting phenomenon that does not exist in the cycle graph with $m=1$. However, we are unable to predict which particular parameters of N and m are related to such asymmetry. Furthermore, in our calculations, we find a large value of the limiting return probability for some special network topology, for instance, on a complete graph in which each pair of nodes is connected, the long-time-averaged return probabilities equal $\chi_{j,j}=(N^2-2N+2)/N^2$ while the other transition probabilities are $\chi_{k,j}=2/N^2$ $(k \neq j)$. This is a striking feature of CTQWs which differs from the properties of the classical counterpart.

ACKNOWLEDGMENTS

The authors would like to thank Zhu Kai for assistance with the software used in the calculations. This work is supported by National Natural Science Foundation of China under Projects No. 10575042 and No. 10775058 and MOE of China under Contract No. IRT0624 (CCNU).

[1] T. Odagaki and M. Lax, Phys. Rev. B **24**, 5284 (1981).
[2] T. Odagaki and M. Lax, Phys. Rev. B **26**, 6480 (1982).
[3] G. H. Weiss, *Aspects and Applications of the Random Walk* (North-Holland, Amsterdam, 1994).
[4] J. Kempe, Contemp. Phys. **44**, 307 (2002).
[5] D. Supriyo, *Quantum Transport: Atom to Transistor* (Cambridge University Press, London, 2005).
[6] A. Ambainis, *Quantum Search Algorithms* (ACM, New York, 2004).
[7] Y. Aharonov, L. Davidovich, and N. Zagury, Phys. Rev. A **48**, 1687 (1993).
[8] N. Shenvi, J. Kempe, and K. Birgitta Whaley, Phys. Rev. A **67**, 052307 (2003).
[9] E. Farhi and S. Gutmann, Phys. Rev. A **58**, 915 (1998).
[10] A. M. Childs, E. Farhi, and S. Gutmann, Quantum Inf. Process. **1**, 35 (2002).
[11] H. Gerhardt and J. Watrous, e-print arXiv:quant-ph/0305182.
[12] N. Konno, Phys. Rev. E **72**, 026113 (2005).
[13] A. Ambainis, J. Kempe, and A. Rivosh, *Coins Make Quantum Walks Faster* (SIAM, Philadelphia, 2005).
[14] D. Shapira, O. Biham, A. J. Bracken, and M. Hackett, Phys. Rev. A **68**, 062315 (2003).
[15] N. Ashwin and V. Ashvin, e-print arXiv:quant-ph/0010117.
[16] G. Abal, R. Siri, A. Romanelli, and R. Donangelo, Phys. Rev. A **73**, 042302 (2006).
[17] D. Solenov and L. Fedichkin, Phys. Rev. A **73**, 012313 (2006).
[18] F. Sorrentino, M. di Bernardo, G. H. Cuéllar, and S. Boccaletti, Physica D **224**, 123 (2006).
[19] H. Krovi and T. A. Brun, Phys. Rev. A **73**, 032341 (2006).
[20] O. Mülken and A. Blumen, Phys. Rev. E **71**, 016101 (2005).
[21] O. Mülken, V. Bierbaum, and A. Blumen, J. Chem. Phys. **124**, 124905 (2006).
[22] O. Mülken and A. Blumen, Phys. Rev. E **71**, 036128 (2005).
[23] A. Volta, O. Mülken, and A. Blumen, J. Phys. A **39**, 14997 (2006).
[24] S. H. Strogatz and I. Stewart, Sci. Am. **269**, 102 (1993).

[25] K. Wiesenfeld, Physica B **222**, 315 (1996).
[26] L. F. Abbott and C. van Vreeswijk, Phys. Rev. E **48**, 1483 (1993).
[27] I. V. Belykh, V. N. Belykh, and M. Hasler, Physica D **195**, 159 (2004).
[28] D. J. Watts and S. H. Strogatz, Nature (London) **393**, 440 (1998).
[29] C. Kittel, *Introduction to Solid State Physics* (Wiley, New York, 1986).
[30] O. Mülken, A. Volta, and A. Blumen, Phys. Rev. A **72**, 042334 (2005).
[31] G. E. Andrews, R. Askey, and R. Roy, *Special Functions* (Tsinghua Univeristy Press, Beijing, China, 2004).
[32] O. Mülken and A. Blumen, Phys. Rev. E **73**, 066117 (2006).
[33] P. C. Richter, Phys. Rev. A **76**, 042306 (2007).